

N th-order coherence of thermal lightJianbin Liu^{1,2,*} and Yanhua Shih¹¹*Department of Physics, University of Maryland Baltimore County, Baltimore, Maryland 21250, USA*²*Photonics Center, College of Physics Science, Nankai University, Tianjin 300071, China*

(Received 4 December 2008; published 18 February 2009)

This paper presents a unified theory for the N th-order ($N \geq 1$) coherence of thermal light. We wish to show that the N th-order coherence or correlation of thermal light is the result of N -photon interference, which involves the superposition of N -photon probability amplitudes, corresponding to different yet indistinguishable ways of triggering a N -photon joint detection event. The near-field third-order spatial coherence of thermal light is calculated and its use suggested for verifying the N -photon interference theory.

DOI: [10.1103/PhysRevA.79.023819](https://doi.org/10.1103/PhysRevA.79.023819)

PACS number(s): 42.50.Ar, 03.65.Ta, 42.50.Dv

I. INTRODUCTION

The discovery and study of light interference played an important role in the history of physical science. It was the observations of the interference phenomenon that provided a solid foundation for the establishment and development of the classical wave theory of light. The quantum theory of light was introduced in the beginning of 1900s [1], and initiated the revolutionary quantum view of the physical world. Almost immediately, the wave-particle and/or particle-wave nature of photons moved into the classical wave theory of interferometry. The historical “which-path” or “both-path” debate between Einstein and Bohr about the path of a photon when passing through an interferometer revealed these concerns [2]. Perhaps Dirac was the first physicist who formulated the viewpoint of quantum mechanics on interference, summarized in his vivid statement: “[A] photon ... only interferes with itself. Interference between two different photons never occurs” [3].

The quantum theory of the second- and higher-order coherence of light was introduced in 1963 by Glauber [4], enlightened by the discovery of Hanbury Brown and Twiss (HBT) of 1956 [5]. The nontrivial second-order temporal and spatial correlations of thermal light observed in a HBT interferometer created quite a surprise and led to a debate about the classical or quantum nature of the phenomena [6]. Although the HBT experiment initiated a number of key concepts of modern quantum optics and prepared an experimental background for the quantum-mechanical photodetection theory, the HBT phenomenon itself was finally interpreted as the statistical correlation of intensity fluctuations and considered as a classical effect. It was believed that the nontrivial HBT correlation is caused by the locally measured intensity fluctuations of the radiation: when the detection of the two photodetectors measures the same mode within the coherence time of the radiation, the photodetectors experience identical intensity fluctuations; therefore, the statistical correlation of the intensity fluctuation achieves its maximum value, which is twice greater than the value when the two photon detection events are triggered by different modes or at a temporal separation greater than the coherence time [7].

Fifty years after the discovery of HBT, in 2006, Scarcelli *et al.* created another surprise by a set of near-field lensless ghost imaging experiments with chaotic thermal light [8]. The ghost imaging experiments showed that nontrivial correlation of thermal light is observable in an experiment in which the two photodetectors have much greater chances to be triggered by different modes than an identical mode at any position of the photodetectors. Following the historical classical interpretation of HBT, there is no chance to observe any nontrivial correlation under the experimental conditions of near-field lensless ghost imaging. What is the cause of the thermal light ghost imaging? We may have to reexamine the standard classical interpretation of HBT, and ask a question: “Can two-photon correlation of chaotic light be considered as a correlation of intensity fluctuations?” [8,9]. Or, to bring back the question we have been facing for half a century since HBT: Is the N th-order ($N \geq 2$) coherence observed in joint detection of distant photodetectors a classical statistical correlation of locally measured intensity fluctuations or a quantum nonlocal multiphoton interference phenomenon?

Although questions regarding the quantum or classical nature behind the second-order coherence or correlation of thermal light still exist [8–14], the N th-order coherence or correlation has shown attractive properties in practical applications. Multiphoton imaging with thermal light is one of these exciting areas. As for the entangled multiphoton states [15,16], the surprising nonlocal behavior and promising enhancement of spatial resolution in multiphoton imaging are both practically useful. Referring to the N th-order coherence or correlation, the main attention has been focused on second-order coherence or correlation [8,10–13], with a few recent discussions about third-order spatial correlation [17,18] and multiphoton interference [19] in the far field. Here, in addition to the earlier work, we will discuss the third-order coherence of thermal light in the near field. Based on the detailed discussions of the first-, second-, and third-order coherence, we will generalize our discussions to any N th-order ($N \geq 1$) coherence of thermal light in both the far field and the near field, thus presenting a unified theory of coherence for thermal light.

This paper is organized as follows. We will first introduce the concepts of quantum and classical N th-order coherence or correlation in Sec. II. In Sec. III, we will apply the Glauber photon detection theory to calculate the nontrivial

*ljb@mail.nankai.edu.cn

N th-order coherence and explore the nonlocal N -photon interference nature of the phenomenon. In Sec. IV, we continue to analyze the nonlocal interference nature of the N th-order coherence of thermal light from a different approach. In this approach, we will show that, although the radiation fields are treated classically, the nonlocal superposition of the multiple fields is consistent with that of the quantum N -photon interference. Further discussions on the physics behind the N th-order coherence of thermal light are then given in Sec. V. Before drawing the conclusion, in Sec. VI, we suggest an experiment for measuring the spatial third-order coherence function of thermal light in the near field to verify the N -photon interference theory. Section VII summarizes the conclusions.

II. QUANTUM AND CLASSICAL THEORIES OF N TH-ORDER COHERENCE OR CORRELATION

In the quantum theory of light, the first-order coherence function $G^{(1)}(\mathbf{r},t)$ measures the probability of observing a photon detection event at space-time point (\mathbf{r},t) [4],

$$\begin{aligned} G^{(1)}(\mathbf{r},t) &= \text{tr}[\hat{\rho}E^{(-)}(\mathbf{r},t)E^{(+)}(\mathbf{r},t)] \\ &= \sum_j P_j \langle \psi_j | E^{(-)}(\mathbf{r},t)E^{(+)}(\mathbf{r},t) | \psi_j \rangle \\ &\equiv \sum_j P_j G_j^{(1)}(\mathbf{r},t), \end{aligned} \tag{1}$$

where

$$\hat{\rho} = \sum_j P_j | \psi_j \rangle \langle \psi_j | \tag{2}$$

is the density operator that characterizes the state of the quantized electromagnetic field, and $G_j^{(1)}(\mathbf{r},t)$ is the probability for the j th photon to trigger that event, or the probability of observing that event when the photon is in the state $| \psi_j \rangle$, at (\mathbf{r},t) . The field is treated as in a mixed state. P_j is the probability of the system to be in the state $| \psi_j \rangle$. $E^{(-)}(\mathbf{r},t)$ and $E^{(+)}(\mathbf{r},t)$ are the negative and positive field operators at space-time coordinate (\mathbf{r},t) , respectively. Regarding the concept of the photon, we may consider either (I) a photon in the mixed state of Eq. (2), or (II) an ensemble of distinguishable photons in the mixed state of Eq. (2). In definition I, $G_j^{(1)}(\mathbf{r},t)$ is the probability of observing that photon at (\mathbf{r},t) when it is in the state $| \psi_j \rangle$, and P_j is the probability for that photon to be in the state $| \psi_j \rangle$. In definition II, $| \psi_j \rangle$ is treated as the state of the j th photon. $G_j^{(1)}(\mathbf{r},t)$ is interpreted as the probability of observing the j th photon at (\mathbf{r},t) , and P_j the probability for the j th photon to contribute to the photon detection event. In both cases, the counting rate of a photon counting detector or the photocurrent of an analog photodetector at space-time coordinate (\mathbf{r},t) is proportional to $G^{(1)}(\mathbf{r},t)$. (In the following, we will use definition II.)

In Eq. (1), the first-order coherence function $G^{(1)}(\mathbf{r},t)$ is the sum of $G_j^{(1)}(\mathbf{r},t)$, which measures the probability of the j th photon to be detected at (\mathbf{r},t) . If there exist two or more alternative ways for the j th photon to produce a photon detection event at (\mathbf{r},t) , $G_j^{(1)}(\mathbf{r},t)$ will be nontrivial and deter-

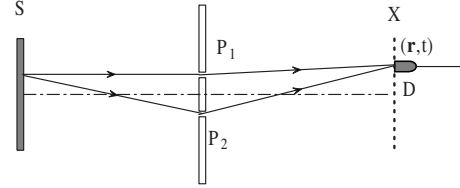


FIG. 1. Young’s double-pinhole interferometer. S stands for the light source; P_1 and P_2 are two pinholes. (\mathbf{r},t) is the space-time point of the single-photon detection event. X is the plane in which the point detector D can scan.

mined by the constructive-destructive superposition of these single-photon probability amplitudes,

$$G_j^{(1)}(\mathbf{r},t) = \left| \sum_k A_k^{(1)}(\mathbf{r},t) \right|^2, \tag{3}$$

where $k=1,2,\dots,M$, and M is the total number of different ways for a photon to trigger a photon detection event. For instance, in Young’s double-pinhole interferometer (Fig. 1) provides two alternative ways for a photon to trigger a photon detection event at (\mathbf{r},t) . The superposition between these two amplitudes, $|A_1^{(1)}+A_2^{(1)}|^2$, determines the probability of observing a photon detection event at space-time coordinate (\mathbf{r},t) . At certain space-time points, the two amplitudes interfere constructively (destructively) and achieve a maximum (minimum) probability. At other space-time points, the interference contributes other values between the maximum and the minimum. The superposition of the two single-photon amplitudes thus yields a nontrivial probability distribution function of (\mathbf{r},t) , namely, an interference pattern. Every photon produces its own interference pattern, and the final observed interference is the sum of all these individual sub-interference patterns.

In the Maxwell electromagnetic wave theory of light, however, the first-order interference is the result of superposition of electromagnetic fields at space-time point (\mathbf{r},t) . In the above Young’s double-pinhole experiment, the observed interference is the result of the superposition at (\mathbf{r},t) between the field E_1 that passes pinhole 1 and the field E_2 that passes pinhole 2, where the intensity $I(\mathbf{r},t)=|E_1+E_2|^2$ is measured by a point photodetector or monitored by an optical instrument such as the human eye. At certain space-time points, E_1 and E_2 interfere constructively (destructively) and achieve a maximum (minimum) intensity. At other space-time points, the interference yields different intensities between the maximum and the minimum. The intensity distribution of light in space-time is therefore a nontrivial function of (\mathbf{r},t) , which is usually recognized as the interference pattern.

Although both quantum and classical theories view the first-order coherence or correlation as interference, the quantum mechanism is quite different from the classical one. As stated by Dirac, quantum theory considers interference a single-photon behavior. The superposed quantum amplitudes belong to a photon. Interference between different photons never occurs, no matter whether in weak light conditions at the single-photon level or in bright light conditions above the classical limit. The classical superposition of fields may involve a large number of photons. For example, in the

Young’s double-pinhole interferometer, it is reasonable to imagine that half of a large number of photons pass pinhole 1 and another half pass pinhole 2. It is quite possible that the classical superposition of $|E_1 + E_2|^2$ means an interference between these two different groups of photons. Unfortunately, it seems impossible to distinguish the quantum picture from the classical one in first-order coherence or correlation measurements. There seems no conclusion, especially in bright light conditions, whether the interference is the result of a photon interfering with itself or one group of photons interfering with another group of photons.

Interestingly and perhaps surprisingly, the difference between quantum and classical mechanisms becomes distinguishable in second- and higher-order coherence or correlation measurements. The second-order coherence function $G^{(2)}(\mathbf{r}_1, t_1; \mathbf{r}_2, t_2)$ measures the probability of observing two photon detection events jointly at space-time points (\mathbf{r}_1, t_1) and (\mathbf{r}_2, t_2) ,

$$\begin{aligned} G^{(2)}(\mathbf{r}_1, t_1; \mathbf{r}_2, t_2) &= \text{tr}[\hat{\rho} E^{(-)}(\mathbf{r}_1, t_1) E^{(-)}(\mathbf{r}_2, t_2) E^{(+)}(\mathbf{r}_2, t_2) E^{(+)}(\mathbf{r}_1, t_1)] \\ &= \sum_j P_j \langle \psi_j | E^{(-)}(\mathbf{r}_1, t_1) E^{(-)}(\mathbf{r}_2, t_2) E^{(+)}(\mathbf{r}_2, t_2) E^{(+)}(\mathbf{r}_1, t_1) | \psi_j \rangle \\ &\equiv \sum_j P_j G_j^{(2)}(\mathbf{r}_1, t_1; \mathbf{r}_2, t_2), \end{aligned} \quad (4)$$

where (\mathbf{r}_1, t_1) and (\mathbf{r}_2, t_2) are the space-time coordinates of the two photon detection events associated with photodetectors D_1 and D_2 , respectively. Again, the density operator $\hat{\rho}$ characterizes the state of the quantized field, which is treated as mixed state. $|\psi_j\rangle$ is the state of the j th jointly measured pair of photons, which may be an entangled state, a product state, or any other type of state. In the chaotic thermal state, the jointly measured pair of photons are completely independent; there is no correlation built into the state. It is only by chance that the two photon detection events occur within a certain time window and this is counted as a “coincidence” or a “joint detection” event. $G_j^{(2)}(\mathbf{r}_1, t_1; \mathbf{r}_2, t_2)$ is interpreted as the probability of observing the j th jointly measured pair of independent photons at (\mathbf{r}_1, t_1) and (\mathbf{r}_2, t_2) , and P_j the probability for the j th pair to contribute to the joint photon detection event. If there exists more than one alternative way for the measured j th pair to trigger a joint detection event at (\mathbf{r}_1, t_1) and (\mathbf{r}_2, t_2) , the superposition of these two-photon amplitudes determines the probability to have the j th joint detection event at (\mathbf{r}_1, t_1) and (\mathbf{r}_2, t_2) . $G_j^{(2)}(\mathbf{r}_1, t_1; \mathbf{r}_2, t_2)$ in Eq. (4) is a result of two-photon interference [8,20],

$$G_j^{(2)}(\mathbf{r}_1, t_1; \mathbf{r}_2, t_2) = \left| \sum_k A_{jk}^{(2)}(\mathbf{r}_1, t_1; \mathbf{r}_2, t_2) \right|^2. \quad (5)$$

For example, the second-order coherence of thermal light observed in the HBT interferometer is calculated from (see Fig. 2)

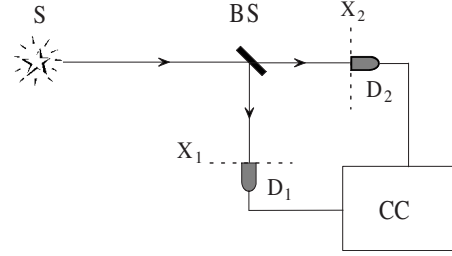


FIG. 2. Schematic of the historical Hanbury Brown and Twiss interferometer which was designed for measuring the angular size of distant stars. S is a far-field thermal source. BS is a 1:1 beam splitter. X_j is the plane in which the point detector D_j can scan ($j = 1, 2$). CC stands for the two-photon coincidence counting system (for photon counting detectors) or twofold linear multiplier (for analog photocurrent detectors).

$$\begin{aligned} G^{(2)}(\mathbf{r}_1, t_1; \mathbf{r}_2, t_2) &= \sum_j |A_{j1}^{(2)} + A_{j2}^{(2)}|^2 \\ &= \sum_j [|A_{j1}^{(2)}|^2 + |A_{j2}^{(2)}|^2 + (A_{j1}^{(2)})^* A_{j2}^{(2)} \\ &\quad + A_{j1}^{(2)} (A_{j2}^{(2)})^*], \end{aligned} \quad (6)$$

where $A_{j1}^{(2)}$ and $A_{j2}^{(2)}$ are the superposed two-photon amplitudes representing two alternative ways for the j th jointly measured pair of independent photons to produce a joint detection event at space-time points (\mathbf{r}_1, t_1) and (\mathbf{r}_2, t_2) , respectively. It is clearly shown in Eq. (6) that the nontrivial correlation function $G^{(2)}(\mathbf{r}_1, t_1; \mathbf{r}_2, t_2)$, i.e., the well-known 50% contrast HBT correlation [21] involves a large number of individual subinterference patterns, where each pattern is produced by a pair of measured independent photons. The two-photon interference occurs within a measured photon pair. Analogous to Dirac’s statement about single-photon interference, we can have a similar statement for two-photon interference: “A photon pair only interferes with itself. Interference between two different photon pairs never occurs.” In certain experimental situations, the two-photon interference occurs at two distant space-time coordinates through the measurement of two photodetectors with two photon detection events at (\mathbf{r}_1, t_1) and (\mathbf{r}_2, t_2) , which can be arranged experimentally to be spacelike separated events. Following Einstein, Podolsky, Rosen (EPR), and Bell [22,23], we name it nonlocal two-photon interference.

In the classical theory of light, the second-order correlation of thermal light is considered as the statistical correlation of the two locally measured intensities $I(\mathbf{r}_1, t_1)$ and $I(\mathbf{r}_2, t_2)$, precisely the correlation of the intensity fluctuations $\Delta I(\mathbf{r}_1, t_1)$ and $\Delta I(\mathbf{r}_2, t_2)$,

$$\begin{aligned} \Gamma_I^{(2)}(\mathbf{r}_1, t_1; \mathbf{r}_2, t_2) &\equiv \langle I_1 I_2 \rangle = \langle (\bar{I}_1 + \Delta I_1)(\bar{I}_2 + \Delta I_2) \rangle \\ &= \bar{I}_1 \bar{I}_2 + \langle \Delta I_1 \Delta I_2 \rangle, \end{aligned} \quad (7)$$

where the ensemble average is based on the statistics of the locally measured intensities $I(\mathbf{r}_1, t_1)$ and $I(\mathbf{r}_2, t_2)$. Obviously, the nontrivial contribution comes from the second term of Eq. (7), $\langle \Delta I_1 \Delta I_2 \rangle$. $\Gamma_I^{(2)}(\mathbf{r}_1, t_1; \mathbf{r}_2, t_2)$ will be a trivial constant $\bar{I}_1 \bar{I}_2$ when the intensity fluctuations are negligible with

$\Delta I_1/I_1 \sim 0$ and $\Delta I_2/I_2 \sim 0$. In classical theory, strictly implementing the locality rules, $I(\mathbf{r}_1, t_1)$ and $\Delta I(\mathbf{r}_1, t_1)$ must be determined by the local field $E(\mathbf{r}_1, t_1)$ only; $I(\mathbf{r}_2, t_2)$ and $\Delta I(\mathbf{r}_2, t_2)$ must be determined by the local field $E(\mathbf{r}_2, t_2)$ only. Classical theory does not allow any nonlocal effect (in EPR-Bell terms), including nonlocal interference.

Traditionally, the statistical correlation of intensity fluctuations is also considered as the statistical correlation of photon number fluctuations. In a HBT interferometer, which is schematically illustrated in Fig. 2, one group of a large number of photons with $N_1 = \bar{N}_1 + \Delta N_1$, fluctuating from time to time, produce photocurrent $i_1(t)$ of D_1 ; another group of photons with $N_2 = \bar{N}_2 + \Delta N_2$, also fluctuating from time to time, produce photocurrent $i_2(t)$ of D_2 . The mean numbers of photons, \bar{N}_1 and \bar{N}_2 , respectively, correspond to the mean intensities of \bar{I}_1 and \bar{I}_2 . The photon number fluctuations ΔN_1 and ΔN_2 , respectively, correspond to the intensity fluctuations ΔI_1 and ΔI_2 . Despite the use of the language of quantum mechanics, in classical theory, the nontrivial HBT correlation is determined by the statistical behavior of two groups of large numbers of photons, independently. The classical mechanism of photon number fluctuation correlation, or the intensity fluctuation correlation, representing the statistical behavior of two groups of a large number of photons, is thus fundamentally different from the two-photon interference picture of the quantum theory, which is based on the quantum-mechanical superposition of two-photon amplitudes within a pair of jointly measured photons. Furthermore, the difference between these two different interpretations is experimentally testable in some conditions, such as when the fluctuations are negligible compared to the mean values. Based on the concept of statistical correlation between locally measured intensity fluctuations, or photon number fluctuations, the second-order correlation function will be a trivial constant in the experimental conditions in which $\Delta I_j/\bar{I}_j \sim 0$ or $\Delta N_j/\bar{N}_j \sim 0$, $j=1,2$. Under the same experimental conditions, however, the quantum theory of two-photon interference will still predict a nontrivial second-order coherence function. A detailed calculation and discussion can be found in Sec. IV.

The N th-order coherence $G^{(N)}(\mathbf{r}_1, t_1; \dots; \mathbf{r}_N, t_N)$ ($N \geq 2$) measures the probability of observing N jointly measured photon detection events at space-time points $(\mathbf{r}_1, t_1), \dots$, and (\mathbf{r}_N, t_N) ,

$$\begin{aligned} G^{(N)}(\mathbf{r}_1, t_1; \dots; \mathbf{r}_N, t_N) &= \text{tr}\{\hat{\rho} E^{(-)}(\mathbf{r}_1, t_1) \cdots E^{(-)}(\mathbf{r}_N, t_N) E^{(+)}(\mathbf{r}_N, t_N) \cdots E^{(+)}(\mathbf{r}_1, t_1)\} \\ &\equiv \sum_j P_j G_j^{(N)}(\mathbf{r}_1, t_1; \dots; \mathbf{r}_N, t_N), \end{aligned} \quad (8)$$

where $G_j^{(N)}(\mathbf{r}_1, t_1; \dots; \mathbf{r}_N, t_N)$ is the contribution from the j th group of jointly measured photons. If there exists more than one alternative way to trigger a joint detection event at $(\mathbf{r}_1, t_1), \dots$, and (\mathbf{r}_N, t_N) , the superposition of these N -photon amplitudes determines the probability to have the j th joint detection event at $(\mathbf{r}_1, t_1), \dots$, and (\mathbf{r}_N, t_N) . $G_j^{(N)}(\mathbf{r}_1, t_1; \dots; \mathbf{r}_N, t_N)$ in Eq. (8) can be written as a superpo-

sition of these N -photon amplitudes $A_k^{(N)}(\mathbf{r}_1, t_1; \dots; \mathbf{r}_N, t_N)$, where $k=1, \dots, M$ and M is the total number of alternative ways for the j th group of photons to trigger the joint detection event at $(\mathbf{r}_1, t_1), \dots$, and (\mathbf{r}_N, t_N) ,

$$G_j^{(N)}(\mathbf{r}_1, t_1; \dots; \mathbf{r}_N, t_N) = \left| \sum_k A_k^{(N)}(\mathbf{r}_1, t_1; \dots; \mathbf{r}_N, t_N) \right|^2. \quad (9)$$

The coincidence counting rate of the N -point photon counting detectors, or the output current of an N -fold linear multiplier which responds linearly to the product of the output currents of N -point photodetectors located at $\mathbf{r}_1, \dots, \mathbf{r}_N$, respectively, is proportional to $G^{(N)}(\mathbf{r}_1, t_1; \dots; \mathbf{r}_N, t_N)$, which sums all the individual contributions of $G_j^{(N)}(\mathbf{r}_1, t_1; \dots; \mathbf{r}_N, t_N)$.

In the classical theory, the N th-order intensity correlation function $\Gamma_j^{(N)}(\mathbf{r}_1, t_1; \dots; \mathbf{r}_N, t_N)$ measures the correlation of N locally measured intensities at space-time points $(\mathbf{r}_1, t_1), \dots$, (\mathbf{r}_N, t_N) , respectively,

$$\Gamma_j^{(N)}(\mathbf{r}_1, t_1; \dots; \mathbf{r}_N, t_N) \equiv \langle I(\mathbf{r}_1, t_1) \cdots I(\mathbf{r}_N, t_N) \rangle. \quad (10)$$

Again, $\langle \cdots \rangle$ denotes an ensemble average based on the statistics of the intensities $I(\mathbf{r}_1, t_1), \dots, I(\mathbf{r}_N, t_N)$, which are measured by photodetectors D_1, \dots, D_N at space-time coordinates $(\mathbf{r}_1, t_1), \dots, (\mathbf{r}_N, t_N)$, locally, independently, and respectively.

III. THE N TH-ORDER COHERENCE FUNCTION: N -PHOTON INTERFERENCE?

In the last section, we have given the definitions of N th-order coherence or correlation based on quantum theory and classical theory. In this section and the next section, we will use these two different definitions to calculate the N th-order coherence or correlation of thermal light.

In this section, we start from the definition of the N th-order coherence function $G^{(N)}(\mathbf{r}_1, t_1; \dots; \mathbf{r}_N, t_N)$ based on Glauber's photodetection theory [4] which is given in Eq. (8). Calculating the N th-order coherence function of thermal light, we model the light source as a large collection of two-level atomic transitions which spontaneously emit radiation independently and randomly [1]. A detailed analysis can be found in Appendix A. The density matrix of thermal light can be formally written as [20,24,25]

$$\hat{\rho} = \sum_{\{n\}} P(\{n\}) |\{n\}\rangle \langle \{n\}|, \quad (11)$$

where

$$|\{n\}\rangle = |n(\mathbf{k}_1)\rangle |n(\mathbf{k}_2)\rangle \cdots |n(\mathbf{k}_N)\rangle$$

is the multimode Fock state with occupation number $n(\mathbf{k}_j)$ for the j th mode, which may take any value from 0 to infinity. \mathbf{k}_j is the wave vector of the j th mode ($j=1, 2, \dots, N$). $P(\{n\})$ is the probability to find the thermal field at the state $|\{n\}\rangle$ with a special set of occupation number combination. The sum includes all the possible combinations or possible states of $|\{n\}\rangle$.

In the following discussions, we replace \mathbf{k}_j with the transverse wave vector $\tilde{\mathbf{k}}_j$ and frequency ω_j to specify the j th

mode, which is helpful to simplify the discussions associated with the nontrivial transverse correlation of thermal light that will be given later as an example. For the same purpose, we write the field operator at the coordinate of the j th photodetector in the following form [25]:

$$E^{(+)}(\vec{\rho}_j, z_j, t_j) = \int d\omega d\vec{\kappa} e^{-i\omega t_j} g_j(\vec{\kappa}, \omega, \vec{\rho}_j, z_j) a(\vec{\kappa}, \omega), \quad (12)$$

where $\vec{\rho}_j$ and z_j are the transverse [two-dimensional (2D) vector] and longitudinal coordinates of the j th point photodetector, respectively. $a(\vec{\kappa}, \omega)$ is the annihilation operator for mode $(\vec{\kappa}, \omega)$. $g_j(\vec{\kappa}, \omega, \vec{\rho}_j, z_j)$ is the Green's function, which propagates the field of mode $(\vec{\kappa}, \omega)$ from the source to the j th detector. For free propagation [25–27],

$$g(\vec{\rho}_j, z_j; \vec{\kappa}, \omega) = \frac{-i\omega e^{i(\omega/c)z_1}}{2\pi c z_1} \int d\vec{\rho}_s \psi\left(\frac{\omega z_1}{c}, \vec{\rho}_j - \vec{\rho}_s\right) \times a(\vec{\rho}_s) e^{i\varphi(\vec{\rho}_s)} e^{-i\vec{\kappa} \cdot \vec{\rho}_s}, \quad (13)$$

where $\psi(\omega z_1/c, \vec{\rho}_j - \vec{\rho}_s) = e^{i(\omega/2cz_1)|\vec{\rho}_j - \vec{\rho}_s|^2}$ is a Gaussian function. $a(\vec{\rho}_s)$ and $\varphi(\vec{\rho}_s)$ are the amplitude and the phase for the mode $\vec{\kappa}$. $\vec{\rho}_s$ is the two-dimensional vector on the transverse plane s , as shown in Fig. 12. z_1 is the distance between the plane s and j . The single-detector counting rate or the output

photocurrent of the j th photodetector is proportional to $G^{(1)}(\mathbf{r}_j, t_j)$,

$$\begin{aligned} G^{(1)}(\vec{\rho}_j, z_j, t_j) &= \text{tr}[\hat{\rho} E^{(-)}(\vec{\rho}_j, z_j, t_j) E^{(+)}(\vec{\rho}_j, z_j, t_j)] \\ &= \sum_{\{n\}} P(\{n\}) \langle \{n\} | E^{(-)}(\vec{\rho}_j, z_j, t_j) E^{(+)}(\vec{\rho}_j, z_j, t_j) | \{n\} \rangle \\ &= \text{const}, \end{aligned} \quad (14)$$

where we have assumed a large-sized bright thermal source. Although the counting rate or the photocurrent of all single detectors is constant in space-time in this condition, quantum theory does not prevent a nontrivial N th-order coherence function $G^{(N)}(\mathbf{r}_1, t_1; \dots; \mathbf{r}_N, t_N)$ ($N \geq 2$) of thermal radiation. In the following we calculate the second-, third-, and N th-order coherence functions of thermal light. We will attempt a calculation based on a modified HBT interferometer, which is the same as shown in Fig. 2, except the distant star is replaced with a large-sized Fresnel near-field chaotic thermal source that is described previously. The joint detection counting rate of D_1 and D_2 or the output current of the standard HBT linear multiplier is proportional to $G^{(2)}(\mathbf{r}_1, t_1; \mathbf{r}_2, t_2)$. For simplicity, we only consider the spatial correlation by taking $\omega \sim \text{const}$, where the temporal correlation always achieves its maximum. The second-order coherence function in this simplified situation is

$$\begin{aligned} G^{(2)}(\mathbf{r}_1, t_1; \mathbf{r}_2, t_2) &= \sum_{\{n\}} P(\{n\}) \int d\vec{\kappa} d\vec{\kappa}' d\vec{\kappa}'' d\vec{\kappa}''' g^*(\vec{\rho}_1, z_1; \vec{\kappa}) g^*(\vec{\rho}_2, z_2; \vec{\kappa}') g(\vec{\rho}_2, z_2; \vec{\kappa}'') \\ &\quad \times g(\vec{\rho}_1, z_1; \vec{\kappa}''') [\delta(\vec{\kappa} - \vec{\kappa}'') \delta(\vec{\kappa}' - \vec{\kappa}''') + \delta(\vec{\kappa} - \vec{\kappa}''') \delta(\vec{\kappa}' - \vec{\kappa}'')] \\ &= \sum_{\dots, n(\vec{\kappa}) \geq 1, \dots, n(\vec{\kappa}') \geq 1, \dots} n(\vec{\kappa}) n(\vec{\kappa}') P(\{n\}) \int d\vec{\kappa} d\vec{\kappa}' \left| \frac{1}{\sqrt{2}} [g(\vec{\rho}_1, z_1; \vec{\kappa}) g(\vec{\rho}_2, z_2; \vec{\kappa}') + g(\vec{\rho}_1, z_1; \vec{\kappa}') g(\vec{\rho}_2, z_2; \vec{\kappa})] \right|^2, \end{aligned} \quad (15)$$

where $g(\vec{\rho}_1, z_1; \vec{\kappa}) g(\vec{\rho}_2, z_2; \vec{\kappa}')$ is the probability amplitude that a photon in mode $\vec{\kappa}$ goes to detector 1 and a photon in mode $\vec{\kappa}'$ goes to detector 2, and $g(\vec{\rho}_1, z_1; \vec{\kappa}') g(\vec{\rho}_2, z_2; \vec{\kappa})$ is the probability amplitude that a photon in mode $\vec{\kappa}'$ goes to detector 1 and a photon in mode $\vec{\kappa}$ goes to detector 2. The second-order coherence is the result of a superposition between these two probability amplitudes of different ways to trigger a two-photon joint detection event at space-time points (\mathbf{r}_1, t_1) and (\mathbf{r}_2, t_2) , respectively. As stated before, the final observed $G^{(2)}(\mathbf{r}_1, t_1; \mathbf{r}_2, t_2)$ is the sum of all individual subinterference patterns, each of which is produced by a measured pair of independent photons.

Substituting Eq. (13) into Eq. (15) and assuming a constant $a(\vec{\rho}_s)$ and $z_1 = z_2 = d$, the normalized second-order coherence function is (detailed calculations can be found in Appendix B)

$$g^{(2)}(\vec{\rho}_1; \vec{\rho}_2) = 1 + \text{somb}^2\left(\frac{R\omega}{d} \left| \vec{\rho}_1 - \vec{\rho}_2 \right| \right) \sim 1 + \delta(\vec{\rho}_1 - \vec{\rho}_2), \quad (16)$$

where the δ function is an approximation by assuming a large enough thermal source of angular size $\Delta\theta \sim R/d$ and high enough frequency ω , such as a visible light source. We thus obtained a point-to-point correlation on two transverse planes. The contrast of the correlation function is 2:1 as shown in Eq. (16) [5].

The third-order spatial coherence function can be measured by a similar experimental setup as the modified HBT interferometer except that three photodetectors are used for three-photon joint detection. The two-photon joint detection circuit will be replaced by a three-photon coincidence counter or three-fold current correlator (see Fig. 3). Again, we assume constant ω to simplify the discussion. The third-order coherence function is

$$\begin{aligned}
 G^{(3)}(\mathbf{r}_1, t_1; \mathbf{r}_2, t_2; \mathbf{r}_3, t_3) = & \sum_{\dots, n(\vec{\kappa}) \geq 1, \dots, n(\vec{\kappa}') \geq 1, \dots, n(\vec{\kappa}'') \geq 1, \dots} n(\vec{\kappa})n(\vec{\kappa}')n(\vec{\kappa}'') \\
 & \times P(\dots, n(\vec{\kappa}), \dots, n(\vec{\kappa}'), \dots, n(\vec{\kappa}''), \dots) \int d\vec{\kappa} \int d\vec{\kappa}' \int d\vec{\kappa}'' \\
 & \times \left| \frac{1}{\sqrt{6}} [g_1(\vec{\kappa})g_2(\vec{\kappa}')g_3(\vec{\kappa}'') + g_1(\vec{\kappa})g_2(\vec{\kappa}'')g_3(\vec{\kappa}') + g_1(\vec{\kappa}')g_2(\vec{\kappa})g_3(\vec{\kappa}'') + g_1(\vec{\kappa}')g_2(\vec{\kappa}'')g_3(\vec{\kappa}) \right. \\
 & \left. + g_1(\vec{\kappa}'')g_2(\vec{\kappa})g_3(\vec{\kappa}') + g_1(\vec{\kappa}'')g_2(\vec{\kappa}')g_3(\vec{\kappa})] \right|^2, \tag{17}
 \end{aligned}$$

where $g_j(\vec{\kappa})$ is shorthand for $g(\vec{\rho}_j, z_j, \vec{\kappa})$. $g_1(\vec{\kappa})g_2(\vec{\kappa}')g_3(\vec{\kappa}'')$ is the probability amplitude that a photon in mode $\vec{\kappa}$ goes to detector 1, a photon in mode $\vec{\kappa}'$ goes to detector 2, and a photon in mode $\vec{\kappa}''$ goes to detector 3. Other terms in Eq. (17) represent different ways to trigger a three-photon joint detection event. From Eq. (17), we see that the third-order coherence is also the result of a large number of three-photon interferences. Each interference pattern is produced by a superposition of a set three-photon amplitudes corresponding to different yet indistinguishable ways for a measured group of three independent photons to trigger a three-photon joint detection event. The final observed $G^{(3)}(\mathbf{r}_1, t_1; \mathbf{r}_2, t_2; \mathbf{r}_3, t_3)$ is the sum of all individual subinterference patterns of every jointly measured group of three photons. The contrast of the third-order coherence function of thermal light is 6:1, a detailed calculation for $G^{(3)}(\mathbf{r}_1, t_1; \mathbf{r}_2, t_2; \mathbf{r}_3, t_3)$ can be found in Sec. VI.

The above calculations can be easily extended to the N th-order ($N \geq 2$) coherence function, which is measurable in the experimental setup of Fig. 4.

$$\begin{aligned}
 G^{(N)}(\mathbf{r}_1, t_1; \dots; \mathbf{r}_N, t_N) = & \sum_{\dots, n(\vec{\kappa}) \geq 1, \dots, n(\vec{\kappa}''') \geq 1, \dots} n(\vec{\kappa}) \cdots n(\vec{\kappa}''') P(\dots, n(\vec{\kappa}), \dots, n(\vec{\kappa}'''), \dots) \\
 & \times \int d\vec{\kappa} \cdots \int d\vec{\kappa}'''' \left| \frac{1}{\sqrt{N!}} \left(\sum_{\vec{\kappa}, \dots, \vec{\kappa}''''}^M g_1(\vec{\kappa}) \cdots g_N(\vec{\kappa}''') \right) \right|^2, \tag{18}
 \end{aligned}$$

where the last $\vec{\kappa}''''$ represents the N th mode; $\sum_{\vec{\kappa}, \dots, \vec{\kappa}''''}^M$ is the sum of all the probability amplitudes of different yet indistinguishable ways to trigger a N -photon joint detection event, which has $N!$ terms. The method to write all the possible probability amplitudes is to keep the order of the detectors the same, i.e., keep all the numbers $1, 2, \dots, N$ in the same order, and change the modes of these photons, i.e., $\vec{\kappa}, \vec{\kappa}', \dots, \vec{\kappa}''''$. Based on Eq. (18), the N th-order coherence is the result of N -photon interference. The final observed $G^{(N)}(\mathbf{r}_1, t_1; \dots; \mathbf{r}_N, t_N)$ ($N \geq 2$) is the sum of all the subinterference patterns produced by every measured group of N photons. By analogy to the second- and third-order coherence, we can easily find that the contrast of the N th-order coherence function of thermal light is $N! : 1$.

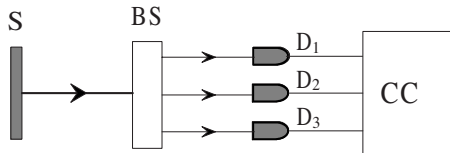


FIG. 3. Experimental setup to measure the third-order spatial coherence function. S is the source. BS is a beam splitter that will split the light into three equal-energy parts. $D_1, D_2,$ and D_3 are three different detectors. CC is a three-photon coincidence count system (for a photon counting detector) or threefold current multiplier (for a photocurrent detector).

IV. THE N TH-ORDER CORRELATION FUNCTION: STATISTICAL CORRELATION OF INTENSITY FLUCTUATIONS?

In this section we attempt a different approach to calculate the N th-order coherence function of bright thermal light in the classical limit. We will do the following.

(I) Calculate the intensity of thermal light locally measured by the j th point photodetector at an arbitrary space-time coordinate (\mathbf{r}_j, t_j) ,

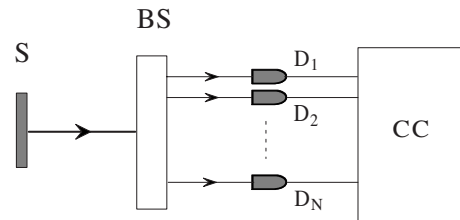


FIG. 4. Experimental setup to measure the N th-order coherence function. S is the source. BS is a beam splitter which will split the light into N equal-energy parts. D_1, D_2, \dots, D_N are N different detectors. CC is an N -photon coincidence count system (for a photon counting detector) or N -fold current correlator (for an analog photocurrent detector).

$$I(\mathbf{r}_j, t_j) \equiv E^*(\mathbf{r}_j, t_j)E(\mathbf{r}_j, t_j),$$

and calculate the N th-order intensity correlation based on the statistics of the N locally measured intensities, respectively at space-time coordinates $(\mathbf{r}_1, t_1), \dots, (\mathbf{r}_N, t_N)$,

$$\Gamma_I^{(N)}(\mathbf{r}_1, t_1; \dots; \mathbf{r}_N, t_N) \equiv \langle I(\mathbf{r}_1, t_1) \cdots I(\mathbf{r}_N, t_N) \rangle. \quad (19)$$

Here, the ensemble average $\langle \cdots \rangle$ means that we take into account all possible realizations of the locally measured intensities.

(II) Compare the result in I with the $2N$ th-order correlation of the fields,

$$\begin{aligned} \Gamma_E^{(N)}(\mathbf{r}_1, t_1; \dots; \mathbf{r}_N, t_N) \\ \equiv \langle E^*(\mathbf{r}_1, t_1)E(\mathbf{r}_1, t_1) \cdots E^*(\mathbf{r}_N, t_N)E(\mathbf{r}_N, t_N) \rangle, \end{aligned} \quad (20)$$

where $E(\mathbf{r}_j, t_j)$ and $E^*(\mathbf{r}_j, t_j)$ are the electric field and its conjugate at space-time coordinate (\mathbf{r}_j, t_j) ($j=1, \dots, N$) [28]. Unlike in Eq. (19), here, $\langle \cdots \rangle$ means that we take into account all possible realizations of the fields, rather than the statistical ensemble average of the locally measured individual intensities. In this calculation the field will be treated classically without quantization, but the classical locality restriction will be released, i.e., allowing the interference between $E(\mathbf{r}_1, t_1)$ and $E(\mathbf{r}_2, t_2)$ through the measurement of two distant photodetectors D_1 and D_2 at (\mathbf{r}_1, t_1) and (\mathbf{r}_2, t_2) .

We assume a thermal source which is bright enough to be considered classical. In this limit, we model the thermal source with a large number of randomly distributed and randomly radiating independent point “subsources,” such as trillions of independent atomic transitions randomly distributed in space and in time, all contribute to the instantaneous intensity [29]. Each point subsorce contributes to the measurement an independent spherical wave as a subfield of complex amplitude $E_j = a_j e^{i\varphi_j}$, where a_j is the real and positive amplitude of the j th subfield and φ_j is a *random* phase associated with the j th subfield. Basically, we have the following pictures for the source: (I) a large number of independent point subsources distributed randomly in space (counted spatially); (II) each point source contains a large number of independently and randomly radiating atoms (counted temporally); (III) a large number of subsources, counted either spatially or temporally, may contribute to each of the independent radiation modes $(\vec{\kappa}, \omega)$ at each of the individual point photodetectors (counted by mode). The instantaneous intensity at space-time (\mathbf{r}_j, t_j) , measured by the j th idealized point photodetector D_j ($j=1, \dots, N$), is calculated as

$$\begin{aligned} I(\mathbf{r}_j, t_j) &= E^*(\mathbf{r}_j, t_j)E(\mathbf{r}_j, t_j) \\ &= \sum_l E_l^*(\mathbf{r}_j, t_j) \sum_m E_m(\mathbf{r}_j, t_j) \\ &= \sum_{l=m} E_l^*(\mathbf{r}_j, t_j)E_l(\mathbf{r}_j, t_j) + \sum_{l \neq m} E_l^*(\mathbf{r}_j, t_j)E_m(\mathbf{r}_j, t_j), \end{aligned} \quad (21)$$

where the subfields are identified by the indices l and m originated from the l and m sub-sources. In Eq. (21) we divided the sum into two groups. The first group represents

the sum of the subintensities, where the l th subintensity originates from the l th subsorce. The second group adds the “cross” terms corresponding to different subsources. When we take into account all possible realizations of the fields, it is easy to find that only the first group, in which the field and its conjugate come from the same subsorce, survives. The second group in Eq. (21) vanishes if $\varphi_l - \varphi_m$ takes all possible values. We may rewrite Eq. (21) into the form of

$$I(\mathbf{r}_j, t_j) = \langle I(\mathbf{r}, t) \rangle + \Delta I(\mathbf{r}, t),$$

where

$$\langle I(\mathbf{r}, t) \rangle \equiv \left\langle \sum_l E_l^*(\mathbf{r}_j, t_j) \sum_m E_m(\mathbf{r}_j, t_j) \right\rangle = \sum_l E_l^*(\mathbf{r}_j, t_j)E_l(\mathbf{r}_j, t_j). \quad (22)$$

The instantaneous intensity $I(\mathbf{r}, t)$ has two contributions: $\langle I(\mathbf{r}, t) \rangle$, which is defined as the expectation value of the intensity, and $\Delta I(\mathbf{r}, t)$, which is defined as the intensity fluctuations. In the classical limit, for thermal light, a large number of independent and randomly radiating subsources contribute to the instantaneous intensity $I(\mathbf{r}_j, t_j)$. This large number of independent randomly distributed subfields may take all possible realizations of their complex amplitudes in the superposition. In this case, and only in this case, the instantaneous intensity takes its expectation value

$$I(\mathbf{r}_j, t_j) \approx \sum_l E_l^*(\mathbf{r}_j, t_j)E_l(\mathbf{r}_j, t_j) = \langle I(\mathbf{r}_j, t_j) \rangle.$$

In a real measurement, especially in weak light conditions, the superposition may not take all possible realizations of the fields and thus results in an incomplete destructive interference. The measured value of $I(\mathbf{r}_j, t_j)$ will be slightly different from its expectation value, causing random fluctuations in the neighborhood of the expectation value from time to time. In the classical limit, however, a large enough number of randomly radiating subsources contribute to the measurement of instantaneous intensity $I(\mathbf{r}_j, t_j)$, negligible random fluctuations are expected with $\Delta I/I \sim 0$. This result is consistent with quantum theory. The thermal state is treated as a mixed state in quantum theory. The Glauber theory of photon detection predicts a constant $G^{(1)}(\mathbf{r}_j, t_j)$, and consequently a constant counting rate of the j th photon counting detector as given in Eq. (14). The constant counting rate corresponds to constant intensity $I(\mathbf{r}_j, t_j)$ measured by the j th photodetector in the classical limit.

Now we calculate $\Gamma_I^{(2)}(\mathbf{r}_1, t_1; \mathbf{r}_2, t_2)$ classically with the help of Eq. (7),

$$\Gamma_I^{(2)}(\mathbf{r}_1, t_1; \mathbf{r}_2, t_2) \equiv \langle I(\mathbf{r}_1, t_1)I(\mathbf{r}_2, t_2) \rangle = \langle I_1 \rangle \langle I_2 \rangle + \langle \Delta I_1 \Delta I_2 \rangle,$$

in which the ensemble average is based on the statistics of each locally measured intensity. In the classical limit, with negligible intensity fluctuations, obviously we obtain

$$\Gamma_I^{(2)}(\mathbf{r}_1, t_1; \mathbf{r}_2, t_2) \approx \bar{I}_1 \bar{I}_2 \sim \text{const.}$$

The classical theory of statistical correlation based on the locally measured random intensity fluctuations does not predict observable nontrivial correlation.

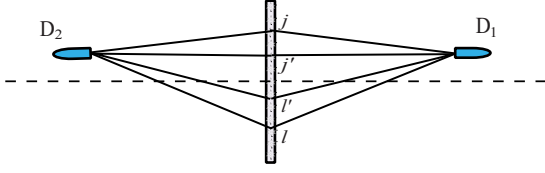


FIG. 5. (Color online) Schematic illustration of $\sum_{j,l}|E_{j1}E_{l2} + E_{l1}E_{j2}|^2$. It is clear that the amplitude pairs $j1 \times l2$ with $l1 \times j2$, where j and l represent all point subsources, pair by pair, will experience equal optical path propagation and superpose constructively when D_1 and D_2 are located at $\vec{\rho}_1 \approx \vec{\rho}_2$, $z_1 \approx z_2$, where $\vec{\rho}_1(z_1)$ and $\vec{\rho}_2(z_2)$ are the transverse (longitudinal) coordinates of D_1 and D_2 .

However, the calculation of the fourth-order correlation of the field, following Eq. (20) by taking $N=2$ gives a different result:

$$\begin{aligned} \Gamma_E^{(2)}(\mathbf{r}_1, t_1; \mathbf{r}_2, t_2) &= \left\langle \sum_{j,k,l,m} E_j^*(\mathbf{r}_1, t_1) E_k(\mathbf{r}_1, t_1) E_l^*(\mathbf{r}_2, t_2) E_m(\mathbf{r}_2, t_2) \right\rangle \\ &= \left\langle \sum_j E_j^*(\mathbf{r}_1, t_1) E_j(\mathbf{r}_1, t_1) \sum_l E_l^*(\mathbf{r}_2, t_2) E_l(\mathbf{r}_2, t_2) \right. \\ &\quad \left. + \sum_j E_j^*(\mathbf{r}_1, t_1) E_j(\mathbf{r}_2, t_2) \sum_l E_l^*(\mathbf{r}_2, t_2) E_l(\mathbf{r}_1, t_1) \right\rangle \\ &= \left\langle \sum_j \sum_l \left| \frac{1}{\sqrt{2}} [E_j(\mathbf{r}_1, t_1) E_l(\mathbf{r}_2, t_2) \right. \right. \\ &\quad \left. \left. + E_l(\mathbf{r}_1, t_1) E_j(\mathbf{r}_2, t_2)] \right|^2 \right\rangle, \end{aligned} \quad (23)$$

where based on the chaotic nature of the independent subsources, after taking into account all possible realizations of the phases associated with the subfields, the only surviving terms in the summation are those with (1) $j=k$, $l=m$, (2) $j=m$, $k=l$. Notice, when claiming the surviving terms $j=m$, $k=l$, we have assumed that the optical radiation fields of $E(\mathbf{r}_1, t_1)$ and $E(\mathbf{r}_2, t_2)$ can interfere with each other through the measurement of two distant independent photodetectors D_1 and D_2 . This postulate is beyond the classical measurement theory of light. Classical theory does not allow any nonlocal effect (in EPR-Bell terms), including nonlocal interference.

It is not difficult to see the nonlocal nature of the superposition shown in Eq. (23). In Eq. (23), $G^{(2)}(\mathbf{r}_1, t_1; \mathbf{r}_2, t_2)$ is written as a superposition between the product of subfields $E_j(\mathbf{r}_1, t_1) E_l(\mathbf{r}_2, t_2)$ and $E_l(\mathbf{r}_1, t_1) E_j(\mathbf{r}_2, t_2)$. The first term in the superposition corresponds to the situation in which the field at D_1 was generated by the j th subsurface, and the field at D_2 was generated by the l th subsurface. The second term in the superposition corresponds to a different yet indistinguishable situation in which the field at D_1 was generated by the l th subsurface, and the field at D_2 was generated by the j th subsurface. Therefore, an interference of $|E_{j1}E_{l2} + E_{l1}E_{j2}|^2$ is concealed in the joint measurement of D_1 and D_2 , which physically occurs at two space-time points (\mathbf{r}_1, t_1) and (\mathbf{r}_2, t_2) . It is easy to see from Fig. 5 the amplitude pairs $j1 \times l2$ with $l1$

$\times j2$, $j'1 \times l'2$ with $l'1 \times j'2$, $j1 \times l'2$ with $l'1 \times j2$, and $j'1 \times l2$ with $l1 \times j'2$, etc., pair by pair, will experience equal total optical path propagation, which involves two arms of D_1 and D_2 , and thus superpose constructively when D_1 and D_2 are placed in the neighborhood of $\vec{\rho}_1 = \vec{\rho}_2$, $z_1 = z_2$, where $\vec{\rho}_1(z_1)$ and $\vec{\rho}_2(z_2)$ are the transverse (longitudinal) coordinates of D_1 and D_2 . Consequently, the summation of these individual constructive interference terms will yield a maximum value. When $\vec{\rho}_1 \neq \vec{\rho}_2$, $z_1 \neq z_2$, however, each pair of the amplitudes may achieve different relative phase and contribute a different value to the summation, resulting in an averaged constant value.

It does not seem to make sense to claim an interference between $[(E_j \text{ goes to } D_1) \times (E_l \text{ goes to } D_2)]$ and $[(E_l \text{ goes to } D_1) \times (E_j \text{ goes to } D_2)]$ in the framework of Maxwell's electromagnetic wave theory of light. This statement is more likely adapted from particle physics, and is more suitable to describe the interference between quantum amplitudes: $[(\text{particle } j \text{ goes to } D_1) \times (\text{particle } l \text{ goes to } D_2)]$ and $[(\text{particle } l \text{ goes to } D_1) \times (\text{particle } j \text{ goes to } D_2)]$, rather than waves. Classical waves do not behave in such a way. In fact, in this model each subsurface corresponds to an independent spontaneous atomic transition in nature, and consequently corresponds to the creation of a photon. Therefore, the above superposition corresponds to the superposition between two indistinguishable two-photon amplitudes, and is thus called *two-photon interference*. Although we started with a model which is in the "classical" limit of the bright light condition, the model of interference between subfields originating from a large number of chaotic point subsources is consistent with the theory of Dirac.

Similar to the quantum calculation, we attempt a near-field calculation to derive the nontrivial correlation of $\Gamma_E^{(2)}(\vec{\rho}_1, z_1; \vec{\rho}_2, z_2)$. We start from Eq. (23) and concentrate on the transverse spatial correlation by taking the frequency ω as a constant. In the near field we apply the Fresnel approximation as usual to propagate the field from each subsurface to the photodetectors. $\Gamma_E^{(2)}(\vec{\rho}_1, z_1; \vec{\rho}_2, z_2)$ can be formally written in terms of the Green's function,

$$\begin{aligned} \Gamma_E^{(2)}(\vec{\rho}_1, z_1; \vec{\rho}_2, z_2) &= \left\langle \int d\vec{k} d\vec{k}' \left| \frac{1}{\sqrt{2}} [g(\vec{\rho}_1, z_1, \vec{k}) g(\vec{\rho}_2, z_2, \vec{k}') \right. \right. \\ &\quad \left. \left. + g(\vec{\rho}_2, z_2, \vec{k}) g(\vec{\rho}_1, z_1, \vec{k}')] \right|^2 \right\rangle \\ &= \left\langle \int d\vec{k} |g(\vec{\rho}_1, z_1, \vec{k})|^2 \int d\vec{k}' |g(\vec{\rho}_2, z_2, \vec{k}')|^2 \right. \\ &\quad \left. + \left| \int d\vec{k} g^*(\vec{\rho}_1, z_1, \vec{k}) g(\vec{\rho}_2, z_2, \vec{k}) \right|^2 \right\rangle \\ &\equiv \Gamma_E^{(1)}(\vec{\rho}_1, z_1; \vec{\rho}_1, z_1) \Gamma_E^{(1)}(\vec{\rho}_2, z_2; \vec{\rho}_2, z_2) \\ &\quad + |\Gamma_E^{(1)}(\vec{\rho}_1, z_1; \vec{\rho}_2, z_2)|^2. \end{aligned} \quad (24)$$

In Eq. (24) we have formally written $\Gamma_E^{(2)}$ in terms of the first-order (second-order in field) correlation functions $\Gamma_E^{(1)}$, but keep in mind that the first-order correlation function $\Gamma_E^{(1)}$ and the second-order (fourth-order in field) correlation function $\Gamma_E^{(2)}$ represent different physics based on different

measurements. Substituting the Green's function of Eq. (13) for free propagation into Eq. (24), we obtain $\Gamma_E^{(1)}(\vec{\rho}_1, z_1)\Gamma_E^{(1)}(\vec{\rho}_2, z_2) \sim \text{const}$ and

$$\begin{aligned} & |\Gamma_E^{(1)}(\vec{\rho}_1, z_1; \vec{\rho}_2, z_2)|^2 \\ & \propto \left| \int d\vec{\rho}_0 a^2(\vec{\rho}_0) e^{-i(\omega/2cd)|\vec{\rho}_1 - \vec{\rho}_0|^2} e^{i(\omega/2cd)|\vec{\rho}_2 - \vec{\rho}_0|^2} \right|^2 \\ & \propto \left| e^{-i(\omega/2cd)(|\vec{\rho}_1|^2 - |\vec{\rho}_2|^2)} \int d\vec{\rho}_0 a^2(\vec{\rho}_0) e^{i(\omega/cd)(\vec{\rho}_1 - \vec{\rho}_2) \cdot \vec{\rho}_0} \right|^2 \\ & \propto \text{somb}^2\left(\frac{R\omega}{d} |\vec{\rho}_1 - \vec{\rho}_2|\right), \end{aligned} \quad (25)$$

where we have assumed $a^2(\vec{\rho}_0) \sim \text{const}$, and $z_1 = z_2 = d$. The transverse spatial correlation function $\Gamma_E^{(2)}(\vec{\rho}_1; \vec{\rho}_2)$ is thus

$$\Gamma_E^{(2)}(|\vec{\rho}_1 - \vec{\rho}_2|) = I_0^2 \left[1 + \text{somb}^2\left(\frac{R\omega}{d} |\vec{\rho}_1 - \vec{\rho}_2|\right) \right]. \quad (26)$$

Consequently, the degree of the second-order spatial coherence is

$$g_E^{(2)}(|\vec{\rho}_1 - \vec{\rho}_2|) = 1 + \text{somb}^2\left(\frac{R\omega}{d} |\vec{\rho}_1 - \vec{\rho}_2|\right) \sim 1 + \delta(|\vec{\rho}_1 - \vec{\rho}_2|), \quad (27)$$

for a large value of $2R/d \sim \Delta\theta$, where $\Delta\theta$ is the angular size of the radiation source viewed at the photodetectors. We effectively have a "point-to-point" correlation between the Fresnel near-field transverse planes of $z_1 = d$ and $z_2 = d$.

We have thus derived the same second-order coherence or correlation function as that of the quantum theory. There is no surprise in having such a result. Although the fields are not quantized, this model has implied the same two-photon interference (nonlocal) mechanism as that of the quantum theory. We may name this model "semiclassical." Unlike the phenomenological theory of intensity fluctuations, this semiclassical model explores the physical cause of the phenomenon [30].

Situations are similar when we consider the third-order coherence or correlation of thermal light. The third-order intensity correlation function is calculated by taking $N=3$ in Eq. (19),

$$\begin{aligned} \Gamma_I^{(3)}(\mathbf{r}_1, t_1; \mathbf{r}_2, t_2; \mathbf{r}_3, t_3) &= \langle I(\mathbf{r}_1, t_1) I(\mathbf{r}_2, t_2) I(\mathbf{r}_3, t_3) \rangle \\ &= \langle (\bar{I}_1 + \Delta I_1)(\bar{I}_2 + \Delta I_2)(\bar{I}_3 + \Delta I_3) \rangle \\ &= \bar{I}_1 \bar{I}_2 \bar{I}_3 + \bar{I}_1 \langle \Delta I_2 \Delta I_3 \rangle + \bar{I}_2 \langle \Delta I_3 \Delta I_1 \rangle \\ &\quad + \bar{I}_3 \langle \Delta I_1 \Delta I_2 \rangle + \langle \Delta I_1 \Delta I_2 \Delta I_3 \rangle. \end{aligned} \quad (28)$$

If the intensity fluctuations is negligible comparing with the mean value of the intensity, then

$$\Gamma_I^{(3)}(\mathbf{r}_1, t_1; \mathbf{r}_2, t_2; \mathbf{r}_3, t_3) \approx \bar{I}_1 \bar{I}_2 \bar{I}_3 \sim \text{const}.$$

Thus the intensity fluctuation theory predicts a constant for the third-order coherence function of thermal light in this condition.

The calculation of the sixth-order field correlation $\Gamma_E^{(3)}(\mathbf{r}_1, t_1; \mathbf{r}_2, t_2; \mathbf{r}_3, t_3)$, which is based on the statistics of fields gives a different result,

$$\begin{aligned} \Gamma_E^{(3)}(\mathbf{r}_1, t_1; \mathbf{r}_2, t_2; \mathbf{r}_3, t_3) &= \langle E(\mathbf{r}_1, t_1) E^*(\mathbf{r}_1, t_1) E(\mathbf{r}_2, t_2) E^*(\mathbf{r}_2, t_2) E(\mathbf{r}_3, t_3) E^*(\mathbf{r}_3, t_3) \rangle \\ &= \left\langle \sum_{j,k,l,m,n,p} E_{j1} E_{k1}^* E_{l2} E_{m2}^* E_{n3} E_{p3}^* \right\rangle \\ &= \left\langle \sum_{j,k,l} \left| \frac{1}{\sqrt{6}} (E_{j1} E_{k2} E_{l3} + E_{j1} E_{k3} E_{l2} + E_{j2} E_{k1} E_{l3} \right. \right. \\ &\quad \left. \left. + E_{j2} E_{k3} E_{l1} + E_{j3} E_{k1} E_{l2} + E_{j3} E_{k2} E_{l1}) \right|^2 \right\rangle, \end{aligned} \quad (29)$$

where $E_{\alpha\beta}$ is short for $E_{\alpha}(\mathbf{r}_{\beta}, t_{\beta})$, meaning the field at space-time point $(\mathbf{r}_{\beta}, t_{\beta})$ emitted by the α th subsource. As shown in Sec. VI, $\Gamma_E^{(3)}(\mathbf{r}_1, t_1; \mathbf{r}_2, t_2; \mathbf{r}_3, t_3)$ is not a trivial constant even when the intensity fluctuation is negligible, which contradicts the prediction of Eq. (28). The interference of the products of three electrical fields in Eq. (29), similar to that of the product of two electrical fields in Eq. (23), can be best interpreted by the quantum (particle) concepts, not the fields. Detail discussions about this kind of interference, i.e., three-photon interference, can be found in Sec. V.

We can easily extend our calculations and discussions to any N th-order ($N \geq 2$) coherence of thermal light based on the second- and third-order cases. In summary, the statistical theory of locally measured intensity fluctuations gives a trivial constant N th-order intensity correlation in the case when the intensity fluctuations are negligible,

$$\Gamma_I^{(N)}(\mathbf{r}_1, t_1; \dots; \mathbf{r}_N, t_N) = \bar{I}_1 \bar{I}_2 \dots \bar{I}_N \sim \text{const}.$$

While based on the superposition of the fields, the nontrivial $2N$ th-order field correlation function is calculated to be

$$\Gamma_E^{(N)}(\mathbf{r}_1, t_1; \dots; \mathbf{r}_N, t_N) = \sum_{j,k,l,\dots} \left\langle \left| \frac{1}{\sqrt{N!}} \left(\sum_{N!} E_{j1} E_{k2} E_{l3} \dots \right) \right|^2 \right\rangle, \quad (30)$$

where $\sum_{N!} E_{j1} E_{k2} E_{l3} \dots$ means that we take all possible ways to write the products of N different electrical fields, which has $N!$ terms. The way to write all the $N!$ terms is to keep the order of subsources j, k, l, \dots the same, and change the order of the detectors, i.e., 1, 2, 3, ... as in Eq. (18) of the quantum calculation part. It is easy to see that each term in the sum corresponding to a quantum-mechanical amplitude in which the j, k, l, \dots subfields are measured by the photodetectors 1, 2, 3, ... It is interesting to see a nontrivial $2N$ th-order field correlation function $\Gamma_E^{(N)}(\mathbf{r}_1, t_1; \dots; \mathbf{r}_N, t_N)$ when the intensity fluctuations are negligible, in which condition the N th-order intensity correlation function $\Gamma_I^{(N)}(\mathbf{r}_1, t_1; \dots; \mathbf{r}_N, t_N)$ is a trivial constant.

V. DISCUSSION

Based on the calculation in Secs. III and IV from both the quantum and classical points of view, we conclude that the

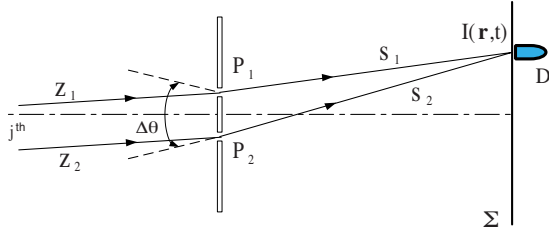


FIG. 6. (Color online) Schematic of an Young's double-pinhole interferometer, which measures the first-order spatial coherence of a thermal radiation generated from a large number of random distributed point sub-sources with an angular size of $\Delta\theta$. The j th photon interfer with itself.

N th-order ($N \geq 2$) coherence or correlation of thermal light is an interference phenomenon. Now we are facing a question: Is the nontrivial correlation the result of quantum or classical interference? For instance, in Eq. (24), the second-order coherence function $\Gamma_E^{(2)}(\mathbf{r}_1, t_1; \mathbf{r}_2, t_2)$ is written in terms of the first-order coherence functions $\Gamma_E^{(1)}(\mathbf{r}_1, t_1; \mathbf{r}_1, t_1)$, $\Gamma_E^{(1)}(\mathbf{r}_2, t_2; \mathbf{r}_2, t_2)$, and $\Gamma_E^{(1)}(\mathbf{r}_1, t_1; \mathbf{r}_2, t_2)$

$$\Gamma_E^{(2)}(\mathbf{r}_1, t_1; \mathbf{r}_2, t_2) = \Gamma_E^{(1)}(\mathbf{r}_1, t_1; \mathbf{r}_1, t_1) \Gamma_E^{(1)}(\mathbf{r}_2, t_2; \mathbf{r}_2, t_2) + |\Gamma_E^{(1)}(\mathbf{r}_1, t_1; \mathbf{r}_2, t_2)|^2.$$

The first-order interference is usually considered as classical interference. The first-order coherence function $\Gamma_E^{(1)}(\mathbf{r}_1, t_1; \mathbf{r}_2, t_2)$ is a quantitative measure of the first-order interference between fields $E(\mathbf{r}_1, t_1)$ and $E(\mathbf{r}_2, t_2)$. Does it mean that the nontrivial $\Gamma_E^{(2)}(\mathbf{r}_1, t_1; \mathbf{r}_2, t_2)$ is a classical superposition of $E(\mathbf{r}, t) = E(\mathbf{r}_1, t_1) + E(\mathbf{r}_2, t_2)$? The answer is negative. In the following we will clarify the different physics behind this $|\Gamma_E^{(1)}(\mathbf{r}_1, t_1; \mathbf{r}_2, t_2)|^2$ and the standard first-order coherence function $\Gamma_E^{(1)}(\mathbf{r}_1, t_1; \mathbf{r}_2, t_2)$ by analyzing the Young's double-pinhole interferometer and the historical HBT experiment. Figure 6 schematically illustrates a Young's double-pinhole interferometer that measures the first-order spatial coherence of the radiation. Assuming a large-sized transverse bright chaotic thermal source consisting of a large number of independent and randomly radiating point sub-sources, the fields $E(\mathbf{r}_1, t_1)$ at pinhole P_1 and $E(\mathbf{r}_2, t_2)$ at pinhole P_2 are treated as the superposition of a large number of independent subfields associated with each subsource. The expectation value of the intensity $I(\mathbf{r}, t)$ on the observation plane Σ is

$$\begin{aligned} \langle I(\mathbf{r}, t) \rangle &= \langle |E(\mathbf{r}, t)|^2 \rangle \\ &= \left\langle \sum_j |E_j(\mathbf{r}_1, t_1) + E_j(\mathbf{r}_2, t_2)|^2 \right\rangle \\ &= \Gamma_E^{(1)}(\mathbf{r}_1, t_1; \mathbf{r}_1, t_1) + \Gamma_E^{(1)}(\mathbf{r}_2, t_2; \mathbf{r}_2, t_2) \\ &\quad + \Gamma_E^{(1)}(\mathbf{r}_1, t_1; \mathbf{r}_2, t_2) + \Gamma_E^{(1)}(\mathbf{r}_2, t_2; \mathbf{r}_1, t_1), \end{aligned} \quad (31)$$

with

$$\Gamma_E^{(1)}(\mathbf{r}_l, t_l; \mathbf{r}_m, t_m) \equiv \left\langle \sum_j E_j^*(\mathbf{r}_l, t_l) E_j(\mathbf{r}_m, t_m) \right\rangle,$$

where the index j labels the point sub-sources, and the indices l and m ($l, m = 1, 2$) label the pinhole P_1 at \mathbf{r}_1 and the pinhole

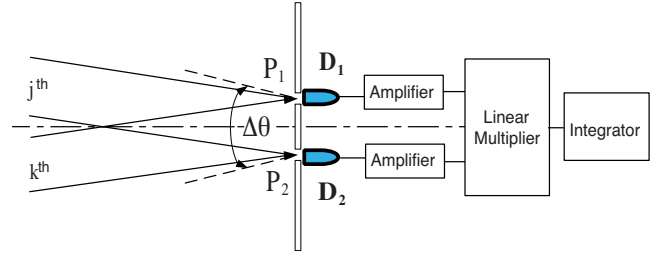


FIG. 7. (Color online) Schematic of a modified Hanbury Brown and Twiss interferometer. The interferometer is similar to the Young's double-pinhole interferometer, except it measures a different interference in the joint detection of two photodetectors. The interference is between the following amplitudes: (1) j th mode to D_1 and k th mode to D_2 , (2) j th mode to D_2 and k th mode to D_1 .

P_2 at \mathbf{r}_2 , and t_1 and t_2 are the early times when the measured radiation passes P_1 and P_2 at $t_1 = t - s_1/c$ and $t_2 = t - s_2/c$. In Eq. (31), an ensemble average has been partially completed by taking into account all possible phases of the subfields. In this experiment, $\Gamma_E^{(1)}(\mathbf{r}_1, t_1; \mathbf{r}_1, t_1)$ measures the interference between "earlier" fields $E(\mathbf{r}_1, t_1)$ and $E(\mathbf{r}_2, t_2)$ at a local space-time point (\mathbf{r}, t) by means of $|E(\mathbf{r}, t)|^2 = |E(\mathbf{r}_1, t_1) + E(\mathbf{r}_2, t_2)|^2$, which is defined as classical interference.

Figure 7 illustrates the historical HBT experiment, which measures the second-order coherence of thermal radiation by two photodetectors at $P_1(\mathbf{r}_1, t_1)$ and $P_2(\mathbf{r}_2, t_2)$. The joint measurement of D_1 and D_2 measures a different interference,

$$\begin{aligned} \Gamma_E^{(2)}(\mathbf{r}_1, t_1; \mathbf{r}_2, t_2) &= \left\langle \sum_j \sum_k \left| \frac{1}{\sqrt{2}} [E_j(\mathbf{r}_1, t_1) E_k(\mathbf{r}_2, t_2) \right. \right. \\ &\quad \left. \left. + E_k(\mathbf{r}_1, t_1) E_j(\mathbf{r}_2, t_2)] \right|^2 \right\rangle \\ &= \Gamma_E^{(1)}(\mathbf{r}_1, t_1; \mathbf{r}_1, t_1) \Gamma_E^{(1)}(\mathbf{r}_2, t_2; \mathbf{r}_2, t_2) \\ &\quad + |\Gamma_E^{(1)}(\mathbf{r}_1, t_1; \mathbf{r}_2, t_2)|^2, \end{aligned}$$

where the indices j and k label the j th and k th point sub-sources. Unlike the first-order correlation function $\Gamma_E^{(1)}(\mathbf{r}_1, t_1; \mathbf{r}_2, t_2)$, here, $|\Gamma_E^{(1)}(\mathbf{r}_1, t_1; \mathbf{r}_2, t_2)|^2$ measures the interference between the two-photon amplitudes. The two-photon amplitudes correspond to a two-photon joint detection event, which are detected by two different detectors at two different space-time coordinates. The two fields $E(\mathbf{r}_1, t_1)$ and $E(\mathbf{r}_2, t_2)$ in the second-order measurement are not superposed at one space-time point.

Unlike the classical first-order interference, the second-order interference cannot be interpreted as classical interference. It is a result of quantum two-photon interference. This conclusion can be easily extended to the N th-order ($N \geq 2$) interference: the N th-order interference is a result of quantum N -photon interference. In the following, we will summarize the quantum interference nature behind the first-, second- and third-order coherence based on the calculations and discussions before, then we will generalize our discussion and conclusions to any N th-order coherence of thermal light.

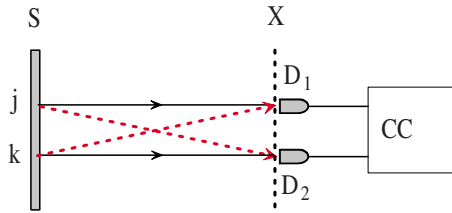


FIG. 8. (Color online) Two-photon interference. S is the thermal source. j and k are the j th and k th atomic transitions, respectively. The two parallel lines represent one way to trigger a joint detection event, and the two crossed lines represent another way to trigger the same joint detection event.

A. The first-order coherence

The first-order coherence gives a quantitative evaluation of the first-order interference that is usually produced by an interferometer. The interferometer introduces two (or more than two) different light paths for creating a photon detection event at a photodetector. As pointed out in the Introduction, although both quantum and classical theories view the first-order coherence as an interference effect, quantum theory treats it as a single photon’s behavior, while classical theory treats it as the interference of classical fields, which can be reasonably considered as the interference of two groups of photons. In quantum theory, the final observed interference pattern of thermal light is the sum of the subinterference patterns produced by each single photon associated with an atomic transition of the source; and the subinterference pattern is the result of a superposition between single-photon probability amplitudes, corresponding to different yet indistinguishable ways for a photon to trigger a photon detection event. Interference occurs if and only if more than one single-photon amplitude is involved in the measurement of a photodetector [31].

B. The second-order coherence

The second-order coherence gives a quantitative evaluation of the second-order interference, instead of the statistical correlation of locally measured intensity fluctuations. As discussed before, quantum theory considers the second-order coherence of thermal radiation as a two-photon interference effect. It is different from the classical intensity fluctuation or photon number fluctuation theory, where it is reasonable to treat the second-order coherence of thermal light as a statistical behavior of two groups of large numbers of photons. The two-photon interference occurs between different two-photon amplitudes belonging to a measured pair of independent photons, and the finally observed nontrivial correlation function is the sum of a large number of these subinterference patterns.

A schematic picture of two-photon interference is illustrated in Fig. 8. There are two different ways for a measured pair of independent photons to trigger a two-photon joint detection event. For instance, the two parallel lines represent one way that the photon emitted by the j th atom goes to detector 1 and the photon emitted by the k th atom goes to detector 2. The two crossed lines represent another way to

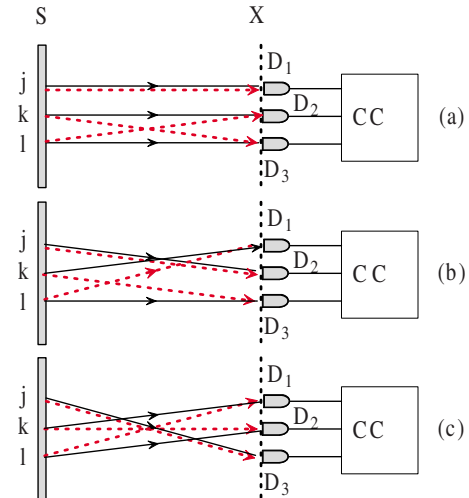


FIG. 9. (Color online) Three-photon interference. S is the source. j , k , and l are the j th, k th, and l th subsources, respectively. There exist six different yet indistinguishable alternative ways of triggering a three-photon joint detection event, described in (a), (b), and (c).

trigger a two-photon joint detection event. Two-photon interference occurs if and only if there exists more than one way for the measured pair to trigger a joint detection event. The final observed second-order correlation is the sum of all these subinterference patterns, each produced by a jointly measured pair of independent photons.

It is worth emphasizing that the two-photon interference means the interference between two-photon probability amplitudes, which is not the interference between two independent photons. The two concepts are fundamentally different.

C. The third-order coherence

The third-order coherence gives a quantitative evaluation of the third-order interference. Quantum theory considers the third-order coherence a three-photon interference effect, which is the result of superposition of three photon amplitudes, corresponding to different yet indistinguishable alternative ways of triggering a three-photon joint detection event at space-time points (\mathbf{r}_1, t_1) , (\mathbf{r}_2, t_2) , and (\mathbf{r}_3, t_3) . It is a behavior of a jointly measured group of three independent photons. The final observed nontrivial third-order correlation is the sum of these subinterference patterns; each is produced by a jointly measured group of three independent photons. Interference between different measured three-photon groups never occurs.

A schematic diagram of three-photon interference is illustrated in Fig. 9. The six different three-photon probability amplitudes shown in (a), (b), and (c) correspond to six alternative ways of triggering a three-photon joint detection event. For instance, the three parallel lines in (a) represent the probability amplitude: a photon emitted from the j th atom goes to detector 1, a photon emitted from the k th atom goes to detector 2, and a photon emitted from the l th atom goes to detector 3. If these six alternatives are indistinguishable, three-photon interference is observable. The three-

photon interference is more complicated than the two-photon interference since the use of three individual photodetectors resulting in six three-photon amplitudes contribute to a three-photon joint detection event. Further discussions about three-photon interference can be found in Sec. VI.

It is also worth noting that three-photon interference does not mean interference between three independent photons.

D. The N th-order coherence:

The N th-order coherence gives a quantitative evaluation of the N th-order interference. All basic concepts developed in the second- and third-order coherence of thermal light can be extended to the the general N th-order ($N \geq 2$) coherence of thermal light. In quantum theory, the N th-order coherence is caused by N -photon interference. The interference is between the N -photon amplitudes within a group of jointly measured N independent photons. The final observed non-trivial N th-order correlation is the sum of a large number of these individual interference patterns; each is produced by an individual group of jointly measured N independent photons.

In summary, we have developed a unified theory for the N th-order coherence of thermal light based on the concept of N -photon interference, which is valid in both the far and near fields for any N -fold joint measurement of photodetectors.

VI. EXPERIMENT: THIRD-ORDER SPATIAL COHERENCE OF THERMAL LIGHT IN THE NEAR FIELD

From the discussions above, it is possible to distinguish quantum multiphoton interference from classical statistical correlation of locally measured intensity fluctuations. In this regard, we have designed an experiment which measures the third-order transverse spatial coherence function in near-field detection planes of a large-sized angular bright thermal source. In these planes, both classical theory and quantum theory predict a constant intensity distribution with negligible intensity fluctuations. Under this condition, classical theory, in which locality is reinforced, gives a trivial constant third-order correlation function $\Gamma_I^{(3)}(\mathbf{r}_1, t_1; \mathbf{r}_2, t_2; \mathbf{r}_3, t_3)$. However, the constant distribution of intensities, measured by each individual photodetector, do not prevent quantum theory predicts a non-trivial third-order coherence function $G^{(3)}(\mathbf{r}_1, t_1; \mathbf{r}_2, t_2; \mathbf{r}_3, t_3)$ in the joint detection of three photodetectors.

The experimental setup of measuring the third-order coherence function is shown in Fig. 10. The three-photon joint detection can be implemented at the photon counting level by means of a three-photon coincidence counter or at higher intensities by using a threefold correlator or rf mixer. Based on Eq. (17) and in Fresnel near-field approximation [25–27], with the condition of $d_1=d_2=d_3$ (d_i is the distance between the source and the detector D_i , $i=1, 2$, and 3; see Fig. 12), the normalized third-order coherence function measured in 1D turns out to be (detailed derivations can be found in Appendix B)

$$g^{(3)}(x_1, t_1; x_2, t_2; x_3, t_3) \propto 1 + \text{sinc}^2\left(\frac{\pi\Delta\theta}{\lambda}(x_1 - x_2)\right) + \text{sinc}^2\left(\frac{\pi\Delta\theta}{\lambda}(x_2 - x_3)\right) + \text{sinc}^2\left(\frac{\pi\Delta\theta}{\lambda}(x_3 - x_1)\right)$$

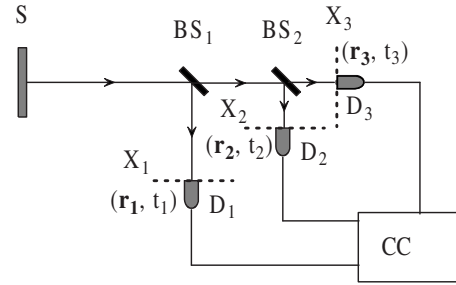


FIG. 10. Experimental setup to measure the third-order spatial coherence function. S is the thermal radiation source consisting of a large number of point subsources. X_j is the transverse plane for the point detector D_j ($j=1, 2$, and 3) to scan. BS_1 is a 1:2 beam splitter, BS_2 is a 1:1 beam splitter so that all these three detectors have equal probability to be triggered by a photon emitted from the source. CC stands for a three-photon coincidence counting system (for photon counting detectors) or a threefold linear multiplier (for analog current detectors).

$$+ 2\text{sinc}\left(\frac{\pi\Delta\theta}{\lambda}(x_1 - x_2)\right)\text{sinc}\left(\frac{\pi\Delta\theta}{\lambda}(x_2 - x_3)\right) \times \text{sinc}\left(\frac{\pi\Delta\theta}{\lambda}(x_3 - x_1)\right),$$

where x_j is the position of detector j ($j=1, 2$, and 3). λ is the wavelength and $\Delta\theta$ is the angular size of the source with respect to the detectors. A numerical simulation of $g^{(3)}(x_1, t_1; x_2, t_2; x_3, t_3)$ is given in Fig. 11. In this simulation we have taken $\lambda=532$ nm, $\Delta\theta=1 \times 10^{-3}$.

In Fig. 11, we find that the contrast of the third-order coherence function of thermal light is 6:1. When the three detectors are in symmetrical positions, i.e., $d_1=d_2=d_3$ and $x_1=x_2=x_3$ (1D), the three-photon amplitudes interfere constructively, and the sum of all these constructive subinterferences yields a maximum value of 6 for $g^{(3)}$. When none of the detectors are in the symmetric positions, the sum of all the subinterferences gives a minimum value of 1 for $g^{(3)}$. The final observed nontrivial third-order coherence function in Fig. 11 is the sum of all the individual subinterference pat-

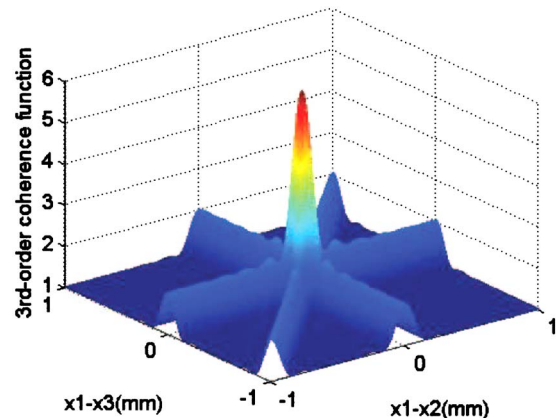


FIG. 11. (Color online) Simulated $g^{(3)}(x_1, t_1; x_2, t_2; x_3, t_3)$ of thermal light in the Fresnel near field. In this simulation we have taken $\lambda=532$ nm, $\Delta\theta=1 \times 10^{-3}$.

terns, which comes from the three-photon interference of every jointly measured group of three independent photons.

VII. CONCLUSION

Let us summarize this paper.

(I) We have developed a unified *N*th-order coherence theory of thermal light [32] based on the quantum concept of *N*-photon interference. *N*-photon interference is the result of the superposition of *N*-photon probability amplitudes, which correspond to different, yet indistinguishable, ways of triggering an *N*-photon joint detection event. The jointly measured group of *N* photons interferes only with the group itself. Interference between different groups never occurs.

(II) We have shown that the classical theory of statistical correlation of intensity fluctuations may not be valid in certain experimental conditions when dealing with *N*th-order ($N \geq 2$) optical coherence of thermal light, such as in joint measurements in the near field of a large-sized angular bright thermal source.

(III) The *N*th-order coherence measurement of thermal light will be “robust.” The *N*-photon interference occurs at the quantum level within a group of jointly measured *N* independent photons; the measurement will not lose coherence or correlation under high-loss propagation, but a longer data collection period will be required.

(IV) We have found that the contrast of the *N*th-order coherence of thermal light is $N! : 1$, which means that the maximum visibility of the *N*th-order coherence function of thermal light is $(N! - 1) / (N! + 1)$. The visibility will increase as *N* increases, and is independent of the intensity. Thus in either the photon counting regime or analog photocurrent measurements, we should be able to achieve the same visibility for the *N*th-order coherence of thermal light. If the contrast of a correlation function is considered as the signal-to-noise ratio (SNR), a high SNR is achievable in *N*-fold joint detection of thermal radiation.

ACKNOWLEDGMENTS

The authors wish to thank M. H. Rubin, J. P. Simon, J. M. Wen, G. Q. Zhang, and Y. Zhou for helpful discussions and suggestions. This research was partially supported by the U.S. AFOSR and ARO-MURI program. J.B.L. acknowledges his partial support from the China Scholarship Council.

APPENDIX A: THE STATE OF THERMAL RADIATION

We assume a large-transverse-sized chaotic thermal source consisting of a large number of independent and randomly radiating point subsources. Each point subsurface may also consist of a large number of independent atoms that are ready for two-level atomic transitions in a random manner. Most of the time, the atoms are in their ground state. There is, however, a small chance for each atom to be excited to a higher energy level E_2 ($\Delta E_2 \neq 0$) and later return back to its ground state E_1 . It is reasonable to assume that each atomic transition generates a field in the single-photon state

$$|\Psi\rangle \approx |0\rangle + \epsilon \sum_{\mathbf{k},s} f(\mathbf{k},s) \hat{a}_{\mathbf{k},s}^\dagger |0\rangle, \tag{A1}$$

where $|\epsilon| \ll 1$ is the probability amplitude for the atomic transition, and $f(\mathbf{k},s) = \langle \Psi_{\mathbf{k},s} | \Psi \rangle$ is the probability amplitude for the radiation field to be in the single-photon state of wave number \mathbf{k} and polarization s : $|\Psi_{\mathbf{k},s}\rangle = |1_{\mathbf{k},s}\rangle = \hat{a}_{\mathbf{k},s}^\dagger |0\rangle$. For this simplified two-level system, the density matrix that characterizes the state of the radiation field excited by a large number of possible atomic transitions is thus

$$\begin{aligned} \hat{\rho} &= \prod_{t_{0j}} \left(|0\rangle + \epsilon \sum_{\mathbf{k},s} f(\mathbf{k},s) e^{-i\omega t_{0j}} \hat{a}_{\mathbf{k},s}^\dagger |0\rangle \right) \\ &\times \prod_{t_{0k}} \left(\langle 0| + \epsilon^* \sum_{\mathbf{k}',s'} f(\mathbf{k}',s') e^{i\omega' t_{0k}} \langle 0| \hat{a}_{\mathbf{k}',s'} \right) \\ &\approx \left[|0\rangle + \epsilon \left(\sum_{t_{0j}} \sum_{\mathbf{k},s} f(\mathbf{k},s) e^{-i\omega t_{0j}} \hat{a}_{\mathbf{k},s}^\dagger |0\rangle \right) + \epsilon^2(\dots) \right] \\ &\times \left[\langle 0| + \epsilon^* \left(\sum_{t_{0k}} \sum_{\mathbf{k}',s'} f(\mathbf{k}',s') e^{i\omega' t_{0k}} \langle 0| \hat{a}_{\mathbf{k}',s'} \right) + \epsilon^{*2}(\dots) \right], \end{aligned} \tag{A2}$$

where $e^{-i\omega t_{0j}}$ is a random phase factor associated with the *j*th atomic transition. Since $|\epsilon| \ll 1$, it is a good approximation to keep the necessary lower-order terms of ϵ in Eq. (A2). After summing over t_{0j} (t_{0k}) by taking into account all its possible values, we obtain

$$\begin{aligned} \hat{\rho} &\approx |0\rangle\langle 0| + |\epsilon|^2 \sum_{\mathbf{k},s} |f(\mathbf{k},s)|^2 |1_{\mathbf{k},s}\rangle\langle 1_{\mathbf{k},s}| \\ &+ |\epsilon|^4 \sum_{\mathbf{k},s} \sum_{\mathbf{k}',s'} |f(\mathbf{k},s)|^2 |f(\mathbf{k}',s')|^2 |1_{\mathbf{k},s} 1_{\mathbf{k}',s'}\rangle\langle 1_{\mathbf{k},s} 1_{\mathbf{k}',s'}| \\ &+ \dots \end{aligned} \tag{A3}$$

The generalized solution for an arbitrary quantized thermal field with occupation number from $n_{\mathbf{k},s} = 0$ to $n_{\mathbf{k},s} \gg 1$ can be obtained directly from Eq. (A2) by keeping all higher-order terms. After summing over t_{0j} and t_{0k} the density matrix can be written as

$$\hat{\rho} = \sum_{\{n\}} p_{\{n\}} |\{n\}\rangle\langle \{n\}|, \tag{A4}$$

where $p_{\{n\}}$ is the probability for the thermal field in the state

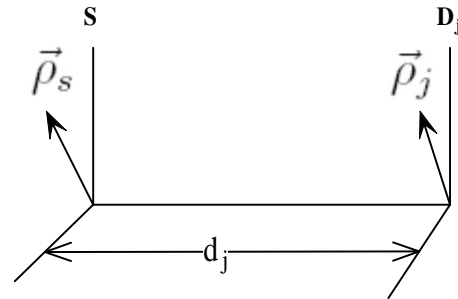


FIG. 12. The relative position between the source and detector *j*, *j* = 1, 2, and 3. ρ_s and ρ_j are the transverse vector in the source plane and the detector *j* plane, respectively. d_j is the distance between the source and the detector *j*.

$$|\{n\}\rangle \equiv \prod_{\mathbf{k},s} |n_{\mathbf{k},s}\rangle = |n_{\mathbf{k},s}\rangle |n_{\mathbf{k}',s'}\rangle \cdots |n_{\mathbf{k}''\cdots,s''\cdots}\rangle.$$

The summation of Eq. (A4) includes all possible modes \mathbf{k} , polarizations s , occupation numbers $n_{\mathbf{k},s}$ for the mode (\mathbf{k},s) and all possible combinations of occupation numbers for different modes in a set of $\{n\}$.

APPENDIX B: THE THIRD-ORDER COHERENCE FUNCTION OF THERMAL LIGHT

Based on the definitions in Refs. [25–27], the Green’s function from the light source to detector j is (see Fig. 12)

$$g_j(\vec{\kappa}) = e^{i(\omega/c)d_j} \psi\left(\vec{\kappa}, -\frac{c}{\omega P_j}\right) e^{i\vec{\kappa}\cdot\vec{\rho}_j}, \quad (\text{B1})$$

where $\psi(\vec{\rho}_j, \omega P_j/c) = e^{i(\omega/2c)P_j} |\vec{\rho}_j|^2$, $P_j = 1/d_j$

We can extend Eq. (B1) to the experimental setup of Fig. 3 by simply changing j to 1, 2, and 3. This corresponds to a separate Green’s function from the source to each of detectors 1, 2, and 3. Now Eq. (17) can be rearranged as

$$\begin{aligned} G^{(3)}(\mathbf{r}_1, t_1; \mathbf{r}_2, t_2; \mathbf{r}_3, t_3) \propto & \int d\vec{\kappa} |g_1(\vec{\kappa})|^2 \int d\vec{\kappa}' |g_2(\vec{\kappa}')|^2 \int d\vec{\kappa}'' |g_3(\vec{\kappa}'')|^2 + \int d\vec{\kappa} |g_1(\vec{\kappa})|^2 \int d\vec{\kappa}' g_2^*(\vec{\kappa}') g_3(\vec{\kappa}') \int d\vec{\kappa}'' g_3^*(\vec{\kappa}'') g_2(\vec{\kappa}'') \\ & + \int d\vec{\kappa}' |g_2(\vec{\kappa}')|^2 \int d\vec{\kappa} g_1^*(\vec{\kappa}) g_3(\vec{\kappa}) \int d\vec{\kappa}'' g_3^*(\vec{\kappa}'') g_1(\vec{\kappa}'') \\ & + \int d\vec{\kappa}'' |g_3(\vec{\kappa}'')|^2 \int d\vec{\kappa} g_1^*(\vec{\kappa}) g_2^*(\vec{\kappa}) \int d\vec{\kappa}' g_2^*(\vec{\kappa}', \omega) g_1(\vec{\kappa}') \\ & + \int d\vec{\kappa} g_1^*(\vec{\kappa}) g_2(\vec{\kappa}) \int d\vec{\kappa}' g_2^*(\vec{\kappa}') g_3(\vec{\kappa}') \int d\vec{\kappa}'' g_3^*(\vec{\kappa}'') g_1(\vec{\kappa}'') \\ & + \int d\vec{\kappa} g_1^*(\vec{\kappa}) g_3(p\vec{a}) \int d\vec{\kappa}' g_2^*(\vec{\kappa}') g_1(\vec{\kappa}') \int d\vec{\kappa}'' g_3^*(\vec{\kappa}'') g_2(\vec{\kappa}''). \end{aligned} \quad (\text{B2})$$

Substituting Eq. (B1) into (B2) and with the condition $d_1=d_2=d_3$ and considering the one-dimensional case, it is easy to get the normalized 1D third-order coherence function by first obtaining the integral of the transverse wave vectors,

$$\begin{aligned} g^{(3)}(x_1, t_1; x_2, t_2; x_3, t_3) \propto & 1 + \text{sinc}^2\left(\frac{\pi\Delta\theta}{\lambda}(x_1 - x_2)\right) + \text{sinc}^2\left(\frac{\pi\Delta\theta}{\lambda}(x_2 - x_3)\right) + \text{sinc}^2\left(\frac{\pi\Delta\theta}{\lambda}(x_3 - x_1)\right) \\ & + 2 \text{sinc}\left(\frac{\pi\Delta\theta}{\lambda}(x_1 - x_2)\right) \text{sinc}\left(\frac{\pi\Delta\theta}{\lambda}(x_2 - x_3)\right) \text{sinc}\left(\frac{\pi\Delta\theta}{\lambda}(x_3 - x_1)\right), \end{aligned} \quad (\text{B3})$$

where $\Delta\theta=2R/d$ is the angular size of the source with respect to the detector plane, and λ is the wavelength. x_j is the position of detector j ($j=1, 2$, and 3). The element $\int d\vec{\kappa} g_j^*(\vec{\kappa}) g_k(\vec{\kappa})$ ($j, k=1, 2, 3$) can be calculated as follows:

$$\begin{aligned} \int d\vec{\kappa} g_j^*(\vec{\kappa}) g_k(p\vec{a}) & = \left(\frac{\omega}{2\pi c}\right)^2 \frac{e^{i(\omega/c)(z_j-z_k)}}{z_j z_k} \int d\vec{\kappa} e^{-i\vec{\kappa}\cdot(\vec{\rho}_s-\vec{\rho}'_s)} \int d\vec{\rho}'_s a^*(\vec{\rho}'_s) e^{-i\varphi(\vec{\rho}'_s)} \\ & \times e^{-i(\omega/2cz_j)|\vec{\rho}_s-\vec{\rho}'_s|^2} \int d\vec{\rho}'_s a(\vec{\rho}'_s) e^{i\varphi(\vec{\rho}'_s)} e^{i(\omega/2cz_k)|\vec{\rho}'_s-\vec{\rho}_k|^2}, \end{aligned} \quad (\text{B4})$$

on the condition of a large enough source,

$$\int d\vec{\kappa} e^{-i\vec{\kappa}\cdot(\vec{\rho}_s-\vec{\rho}'_s)} \sim \delta(\vec{\rho}_s-\vec{\rho}'_s).$$

with substitution of this δ function into Eq. (B4) and on the condition of $z_j=z_k=d$ and $a(\vec{\rho}_s)$ a constant, Eq. (B4) can be simplified as

$$\int d\vec{\kappa} g_j^*(\vec{\kappa}) g_k(p\vec{a}) = \text{somb}\left(\frac{R}{d} \frac{\omega}{c} |\vec{\rho}_j - \vec{\rho}_k|\right),$$

in the 1D case, this can be simplified further to

$$\int d\vec{\kappa} g_j^*(\vec{\kappa}) g_k(\vec{\kappa}) = \text{sinc}\left(\frac{R}{d} \frac{\omega}{c} |x_j - x_k|\right),$$

- [1] R. Loudon, *The Quantum Theory of Light*, 2nd ed. (Oxford University Press, New York, 1983).
- [2] A. J. Wheeler and W. H. Zurek, *Quantum Theory and Measurement* (Princeton University Press, Princeton, NJ, 1983).
- [3] P. A. M. Dirac, *The Principles of Quantum Mechanics*, 4th ed. (Clarendon Press, Oxford, 1958).
- [4] R. J. Glauber, Phys. Rev. **130**, 2529 (1963); **131**, 2766 (1963).
- [5] R. H. Brown and R. Q. Twiss, Nature (London) **177**, 27 (1956); **178**, 1046 (1956).
- [6] R. H. Brown, *Intensity Interferometer* (Taylor and Francis, London, 1974).
- [7] There are two pieces of experimental evidence giving us confidence to believe this “identical-mode”–“different-mode” argument. (1) The joint measurements in the HBT apparatus are in the far-field plane, which is equivalent to the Fourier transform plane. The maximum transverse spatial correlation was indeed observable when the two photodetectors were placed at the positions on the Fourier transform plane corresponding to an identical mode. (2) The maximum temporal correlation was achievable only when applying narrow bandpass filters which select an identical temporal mode for the joint detection of the two photodetectors.
- [8] G. Scarcelli, V. Berardi, and Y. H. Shih, Phys. Rev. Lett. **96**, 063602 (2006).
- [9] A. Valencia, G. Scarcelli, M. D’Angelo, and Y. H. Shih, Phys. Rev. Lett. **94**, 063601 (2005); Giuliano Scarcelli, Vincenzo Berardi, and Yanhua Shih, Appl. Phys. Lett. **88**, 061106 (2006).
- [10] R. S. Bennink, S. J. Bentley, and R. W. Boyd, Phys. Rev. Lett. **89**, 113601 (2002); R. S. Bennink, S. J. Bentley, R. W. Boyd, and John C. Howell, *ibid.* **92**, 033601 (2004).
- [11] A. Gatti, E. Brambilla, M. Bache, and L. A. Lugiato, Phys. Rev. A **70**, 013802 (2004); Phys. Rev. Lett. **93**, 093602 (2004); F. Ferri, D. Magatti, A. Gatti, M. Bache, E. Brambilla, and L. A. Lugiato, *ibid.* **94**, 183602 (2005); A. Gatti, M. Bache, D. Magatti, E. Brambilla, F. Ferri, and L. A. Lugiato, J. Mod. Opt. **53**, 739 (2006).
- [12] Y. J. Cai and S. Y. Zhu, Opt. Lett. **29**, 2716 (2004); Phys. Rev. E **71**, 056607 (2005).
- [13] K. Wang and D. Z. Cao, Phys. Rev. A **70**, 041801(R) (2004); J. Xiong, D. Z. Cao, F. Huang, H. G. Li, X. J. Sun, and K. G. Wang, Phys. Rev. Lett. **94**, 173601 (2005).
- [14] B. I. Erkmen and J. H. Shapiro, Phys. Rev. A **77**, 043809 (2008).
- [15] A. N. Boto, P. Kok, D. S. Abrams, S. L. Braunstein, C. P. Williams, and J. P. Dowling, Phys. Rev. Lett. **85**, 2733 (2000).
- [16] M. D’Angelo, M. V. Chekhova, and Y. H. Shih, Phys. Rev. Lett. **87**, 013602 (2001).
- [17] L. H. Ou and L. M. Kuang, J. Phys. B **40**, 1833 (2007).
- [18] Y. F. Bai and S. S. Han, Phys. Rev. A **76**, 043828 (2007).
- [19] I. N. Agafonov, M. V. Chekhova, T. Sh. Iskhakov, and A. N. Penin, Phys. Rev. A **77**, 053801 (2008).
- [20] M. O. Scully and M. Z. Zubairy, *Quantum Optics* (Cambridge University Press, Cambridge, U.K., 1997).
- [21] 50% contrast means that the ratio of the correlation to the constant background is 2:1. The visibility equals $(2-1)/(2+1)=33.3\%$.
- [22] A. Einstein, B. Poldolsky, and N. Rosen, Phys. Rev. **47**, 777 (1935).
- [23] J. S. Bell, *Speakable and Unsayable in Quantum Mechanics* (Cambridge University Press, New York, 1987).
- [24] L. Mandel and E. Wolf, *Optical Coherence and Quantum Optics* (Cambridge University Press, Cambridge, U.K., 1995).
- [25] Y. Shih, e-print arXiv:0805.1166v1.
- [26] M. H. Rubin, Phys. Rev. A **54**, 5349 (1996).
- [27] J. W. Goodman, *Introduction to Fourier Optics* (McGraw-Hill, New York, 1968).
- [28] The N th-order intensity correlation function and $2N$ th-order field correlation function are different by definition. $\Gamma_I^{(N)}(\mathbf{r}_1, t_1; \dots; \mathbf{r}_N, t_N)$ is defined as the N th-order intensity correlation function, in which the ensemble average is based on the statistics of the locally measured intensities by means of “taking into account all possible realizations of the intensities,” according to Eq. (19). $\Gamma_E^{(N)}(\mathbf{r}_1, t_1; \dots; \mathbf{r}_N, t_N)$ is defined as the $2N$ th-order correlation function of the fields, in which the ensemble average is based on the statistics of the fields by means of “taking into account all possible realizations of the fields,” according to Eq. (20).
- [29] Perhaps this is a necessary experimental condition for simulating a “classical” light source. If a light source can only produce a few photons participating in the measurement, we believe the quantum treatment is an appropriate choice.
- [30] An interesting opinion claims that if a semiclassical theory gives the same result as that of the quantum theory for a physical effect, that physical effect must be classical. We believe the nature of a physical effect is not determined by a theory. One may use a semiclassical theory to calculate the result of a quantum effect. The effect, however, is still quantum. In Wheeler’s opinion, with which this paper is in agreement, “physics is not just calculemus, physics is about the cause behind the calculemus.”
- [31] R. P. Feynman, R. B. Leighton, and M. Sands, *The Feynman Lectures on Physics* (Addison-Wesley, Reading, MA, 1963), Vol. 3.
- [32] A unified theory of N th-order coherence for entangled states based on the concept of N -photon interference and a discussion about the relation between entangled photons and thermal light will be given in a separate presentation.